1 **Performance evaluation of multiple satellite rainfall products for Dhidhessa River Basin**
2 **(DRB), Ethiopia**

3 **Gizachew Kabite Wedajo[a,b*], Misgana Kebede Muleta[c], Berhan Gessesse Awoke[b,d]**

4 [a]Department of Earth Sciences, Wollega University, P.O.Box 395, Nekemte, Ethiopia

5 [b]Department of Remote Sensing, Entoto Observatory Research Center, Ethiopia Space Science
6 Technology Institute, P.O.Box 33679, Addis Ababa, Ethiopia

7 [c]Department of Civil and Environmental Engineering, California Polytechnic State University,
8 San Luis Obispo, California, 93407

9 [d]Department of Geography and Environmental Studies, Kotebe Metropolitan University, Addis
10 Ababa, Ethiopia

11 *Correspondence: Email: Kabiteg@gmail.com

13   *Abstract*

14   *Precipitation is crucial driver of hydrological processes. Ironically, a reliable characterization*

15   *of its spatiotemporal variability is challenging. Ground-based rainfall measurement using rain*

16   *gauges is more accurate. However, installing a dense gauging network to capture rainfall*

17   *variability can be impractical. Satellite-based rainfall estimates (SREs) could be good*

18   *alternatives, especially for data-scarce basins like in Ethiopia. However, SREs rainfall is*

19   *plagued with uncertainties arising from many sources. The objective of this study was to*

20   *evaluate the performance of the latest versions of several SREs products (i.e., CHIRPS2,*

21   *IMERG6, TAMSAT3 and 3B42/3) for the Dhidhessa River Basin (DRB). Both statistical and*

22   *hydrologic modelling approaches were used for the performance evaluation. The Soil and*

23   *Water Analysis Tool (SWAT) was used for hydrological simulations. The results showed that*

24   *whereas all four SREs products are promising to estimate and detect rainfall for the DRB, the*

25   *CHIRPS2 dataset performed the best at annual, seasonal and monthly timescales. The*

26   *hydrologic simulation based evaluation showed that SWAT's calibration results are sensitive*

27   *to the rainfall dataset. The hydrologic response of the basin is found to be dominated by the*

28   *subsurface processes, primarily by the groundwater flux. Overall, the study showed that both*

29   *CHIRPS2 and IMERG6 products could be reliable rainfall data sources for hydrologic*

30   *analysis of the DRB. Moreover, climatic season of the DRB influences rainfall and streamflow*

31   *estimation. Such information is important for rainfall estimation algorithm developers.*

32   ***Keywords:*** *Satellite-based rainfall estimates; Dhidhessa River Basin; Performance evaluation;*

33   *Statistical evaluation; Hydrological modelling performance.*

1. Introduction

Precipitation is an important hydrological component (Behrangi et al., 2011; Meng et al., 2014). Accurate representation of its spatiotemporal variability is crucial to improves hydrological modelling (Grusson et al., 2017). Ironically, precipitation is one of the most challenging hydrometeorological data to be accurately represented (Yong et al., 2014). Climatic and topographic conditions are the primary factors that affect the accuracy of rainfall measurements.

Rainfall is measured either using ground-based (i.e., rain gauge and radar) or satellite sensors, where all measurement methods exhibit limitations (Thiemig et al., 2013). In addition, Commercial Microwave Links (CML) is introduced recently as cheap and fast rainfall estimation method (Smiatek et al., 2017) but not fully tested methodology (Nebuloni et al., 2020). Ground-based rainfall measurements using rain gauge is a direct and generally accurate near the sensor location. However, rain gauges, for instant, either are of poor density to represent spatial and temporal variability of precipitation, or may not even exist in many basins especially in developing countries (Behrangi et al., 2011). Rain gauge based rainfall measurement techniques provide point measurements and subject to missing data due to mainly measurement errors (Kidd et al., 2012; Maggioni et al., 2016). It may also be infeasible to install and maintain dense ground-based gauging stations in remote areas like mountains, deserts, forests and large water bodies (Dinku et al., 2018; Tapiador et al., 2012). On the other hand, radar-based rainfall measurement technique covers larger area and provides rainfall data at high spatial and temporal scales (Sahlaoui and Mordane, 2019). However, radar rainfall measurements have limitations due to attenuation of radar signal by several features that negatively affect the quality of rainfall measurement (Villarini and Krajewski, 2010; Berne and Krajewski, 2013; Sahlaoui and Mordane, 2019). Satellite-based rainfall estimates (SREs), however, provide high-resolution precipitation data including in areas where ground-based rainfall measurements are impractical, sparse, or non-existent (Stisen and Sandholt, 2010).

Consequently, high-resolution precipitation products have been developed over the last three decades. These products include Tropical Rainfall Measuring Mission (TRMM) Multi-satellite Precipitation Analysis (TMPA; Huffman et al., 2007), the Precipitation Estimation from Remote Sensing Information Using Artificial Neuron Networks (PERSIANN; Sorooshian et al., 2000), Climate Prediction Center (CPC) morphing algorithm (CMORPH) (Joyce et al., 2004), African Rainfall Climatology (ARC) (Xie and Arkin 1995), Tropical

Applications of Meteorology using SATellite (TAMSAT) (Maidment et al., 2017) and the Climate Hazards Group InfrareRed Precipitation with Stations (CHIRPS) (Funk et al., 2015). The consistency, spatial coverage, accuracy and spatiotemporal resolution of SREs have been improved over time (Behrangi et al., 2011).

As indirect rainfall estimation techniques, SREs products possess uncertainties resulting from errors in measurement, sampling, retrieval algorithm, and bias correction processes (Dinku et al., 2010; Gebremichael et al., 2014; Tong et al., 2014). Local topography and climatic conditions can also affect the accuracy of SREs estimation (Bitew and Gebremichael, 2011). Hence, SREs products should be carefully evaluated before using the products for any application. Statistical and hydrological modelling are two common methods for evaluating SREs. The statistical evaluation method examines the intrinsic precipitation data quality including its spatiotemporal characteristics via pairwise comparison of the SREs products and ground observations. Scale mismatches between area-averaged SRE data and point-like ground-based measurements is the most critical drawback. The hydrological modelling method evaluates the performance of a SREs product for a specific application such as streamflow predictive ability at watershed scale (Su et al., 2017). The two methods complement each other where the statistical method provides information on data quality while the hydrological model technique assesses the usefulness of the data for hydrological applications (Thiemig et al., 2013). However, most studies used only statistical evaluation methods (e.g., Dinku et al., 2018; Ayehu et al., 2018).

Studies have recommended SREs products for data scare basins (Behrangi et al., 2011; Bitew and Gebremichael, 2011; Thiemig et al., 2013). However, there is no consensus regarding "best" SREs product for different climatic regions. Nesbitt et al. (2008) found that CMORPH and PERSIANN produced higher rainfall rates compared to TRMM for the mountain ranges of Mexico. Dinku et al. (2008) reported better performance of the TRMM and CMORPH products in Ethiopia and Zimbabwe whereas PERSIANN outperformed TRMM in South America according to de Goncalves et al. (2006). Interestingly, the performance of SREs products seems to differ even within a basin. For the Blue Nile basin in Ethiopia, for example, CMORPH overestimated precipitation for the lowland areas but underestimated for the highlands (Bitew and Gebremichael, 2011; Habib et al., 2012; Gebremichael et al., 2014). The discrepancy in the findings of these studies shows the performance of SREs varies with region, topography, season, and climatic conditions of the study area (Kidd and Huffman, 2011;

Seyyedi et al., 2015; Nguyen et al., 2018; Dinku et al., 2018). As such, many studies have recommended SREs evaluation at a local scale to verify its performance for specific applications (Hu et al., 2014; Toté et al., 2015; Kimani et al., 2017; Ayehu et al., 2018).

Studies have examined the performance of SREs in Ethiopia (Haile et al., 2013; Worqlul et al., 2014; Ayehu et al., 2018; Dinku et al., 2018). However, majority of these studies used the statistical method to evaluate SREs, and no study has been completed for the Dhidhessa River Basin (DRB). With only 0.32 rain gauges per 1000 km^2, the DRB meets the World Meteorological Organization (WMO) data-scarce basin classification (WMO, 1994). Evaluating the performance of various SREs products in terms of characterizing the spatiotemporal distribution of rainfall in the DRB could assist with the planning and management of existing and planned water resources projects in the river basin.

SREs have been continuously updated to minimize bias and uncertainty. Evaluating and validating improved products for various climatic regions would be valuable (Kimani et al., 2017). Recently improved SREs products include Tropical Rainfall Measuring Mission (TRMM) Multi-Satellite Precipitation Analysis version 7 (here after referred to as 3B43 for monthly and 3B42 for daily products), Climate Hazards Group InfrareRed Precipitation with Stations version 2 (CHIRPS2), Tropical Applications of Meteorology using SATellite version 3 (TAMSAT3) and Integrated Multi-satellitE Retrievals for GPM version 6B (IMERG6). Studies have reported improvements of these new versions compared to their predecessors. However, to the best of authors' knowledge, the rainfall detection and hydrological simulation capability of these SREs datasets were not evaluated for the basins in Ethiopian including the DRB. This study examined the latest SREs products in terms of their rainfall detection and estimation skills, and improving hydrological prediction for DRB, a medium-sized river basin with scarce gauging data. As such, the objectives of this study were: 1) to evaluate the intrinsic rainfall data quality and detection skills of multiple SREs products (i.e., 3B42/3, CHIRPS2, TAMSAT3, and IMERG6), and 2) to examine hydrologic prediction performances of SREs for the DRB. The Soil and Water Assessment Tool (SWAT), a physically based semi-distributed model that has performed well in humid tropical regions like Ethiopia, was used for the hydrologic simulation.

2. Methods and Materials

2.1. Descriptions of the study area

The Dhidhessa River drains to the Blue Nile River (Figure 1). It is one of the largest and most important river basins in Ethiopia in terms of its physiography and hydrology (Yohannes, 2008). Located between $7°42'43''N$ to $10°2'55''N$ latitude and $35°31'23''E$ to $37°7'60''E$ longitude, the river basin exhibits highly variable topography that ranges from 619 m to 3213 m above mean sea level (a.m.s.l). The Dhidhessa River starts from the Sigmo mountain ranges and travels 494 km before it joins the Blue Nile River around the Wanbara and Yaso districts. The outlet considered for this study is the confluence of the Dhidhessa River and the Blue Nile River which covers a total drainage area of 28,175 km^2. The River basin has many perennial tributaries (Figure 1).

Temperature and precipitation in the Dhidhessa River basin exhibit substantial spatial and seasonal variability. The mean maximum and minimum daily air temperatures in the river basin range from 20-33$°C$ and 6-19 $°C$, respectively. The long-term mean annual rainfall ranges from 1200 mm to 2200 mm in the river basin. Soils in the DRB are generally deep and have high organic content implying they have high infiltration potential. The dominant soil type is Acrisols while Cambisols and Nitisols are common (OWWDSE, 2014). Igneous, sedimentary and metamorphic rocks are common but igneous rock, particularly basalt, is dominant in the basin (GSE, 2000). Forest, shrubland, grassland, and agriculture are the dominant land cover types in the basin (Kabite et al., 2020). Major crops include perennial and cash crops like coffee, Mango, and Avocado (OWWDSE, 2014).

150
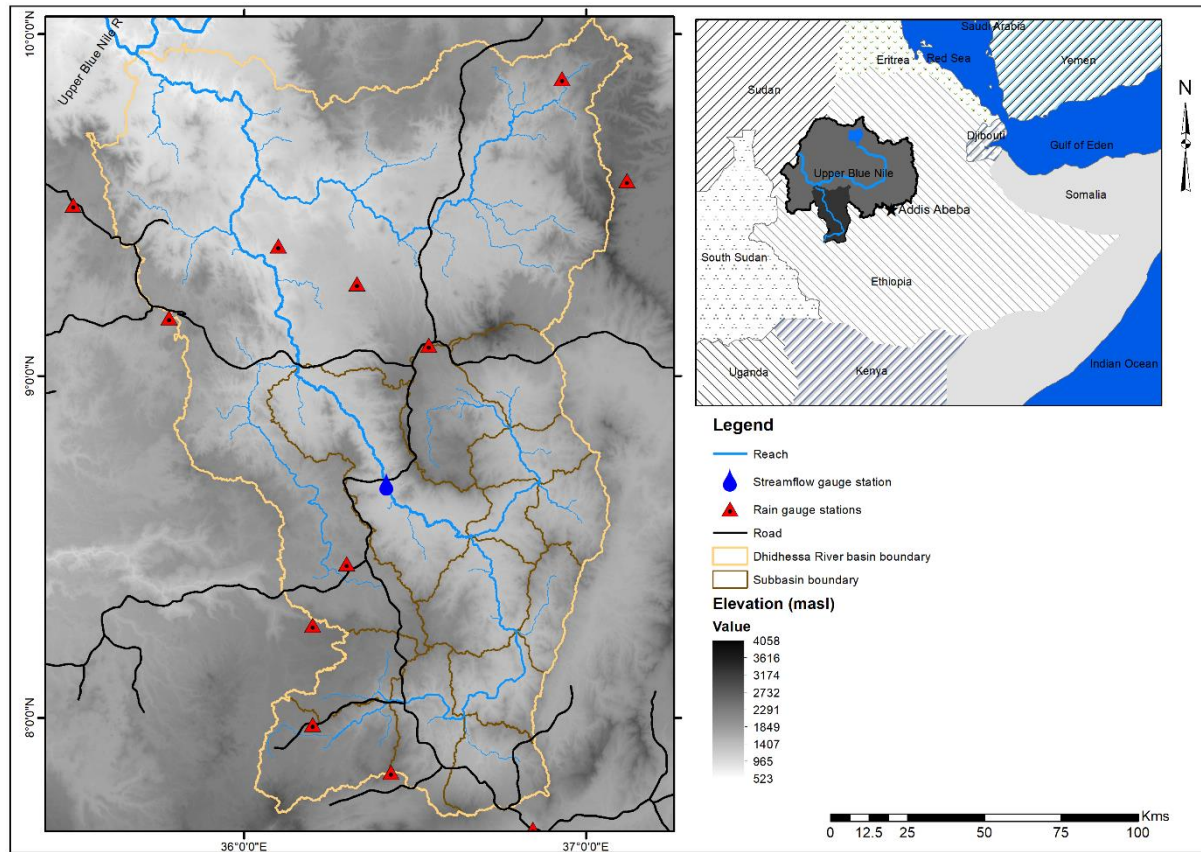
151 Figure 1. Location map of Dhidhessa River basin with ground stations (USGS, 1998).

152 **2.2. Data sources and descriptions**

153 For this study, we used different spatial and temporal datasets such as Digital Elevation

154 Model (DEM), climate, streamflow, soil and land cover from different sources (Table 1).

155 Table 1. Data description and sources.

Data type	Data periods	Resolution	Sources
SRTM DEM	1998	30 * 30 m	USGS
3B42/3	2001-2014	$0.25°$(~25 km)	NASA & JAXA
CHIRPS2	2001-2014	$0.05°$ (~5 km)	USGS & Climate Hazard Group
TAMSAT3	2014-2014	$0.0375°$(~4 km)	Reading University
IMERG6	2001-2014	$0.1°$(~10 km)	NASA & JAXA
Streamflow data	2001-2014	Daily	EMoWI
Meteorological data	2001-2014	Daily	NMA
Land cover	2001	30*30 m	Kabite et al. (2020)
Soil map	2013/14	variable	EMoWI, FAO & OWWDSE

156   Shuttle Radar Thematic Mapper (SRTM) derived Digital Elevation Model (DEM) of

157   30*30 m spatial resolution was obtained from the United States Geological Survey (USGS). It

158   is one of the input data for SWAT model from which topographic and drainage parameters

159   (e.g., drainage pattern, slope and watershed boundary) were derived. Soil map was obtained

160   from source described in Table 1. Soil physical properties required for SWAT model were

161   derived from the soil map. Supervised image classification was used to prepare land cover map

162   of 2001.Together with land cover and soil maps, DEM was used to create Hydrologic Response

163   Units (HRUs).

164   Rainfall data for nine stations within the river basin and for three nearby stations (Figure

165   1), from 2001 to 2014 were obtained from the National Meteorological Agency (NMA) of

166   Ethiopia. The rainfall data was used to evaluate the SREs using the statistical and hydrological

167   modelling evaluation methods. In addition, Enhanced National Climate Time-series Service

168   (ENACTS) gridded (4 m *4 m) minimum and maximum air temperature data was obtained

169   from the National Meteorological Agency (NMA) of Ethiopia. Daily streamflow data from

170   2001 to 2014 was obtained for a station near the town of Arjo (Figure 1) from Ethiopian

171   Ministry of Water, Irrigation and Energy (EMoWI).

172   The hydrometeorological stations used for this study were selected due to their long-

173   term records and better data quality. The observed streamflow was used to calibrate and

174   validate SWAT model. Land use map for 2001 and soil map were obtained from Kabite et al.

175   (2020) and Ethiopian Ministry of Water, Irrigation and Energy (EMoWI), respectively.

2.2.1. Satellite rainfall products

177   The Satellite Rainfall Estimates (SREs) considered in this study include 3B42/3,

178   TAMSAT3, CHIRPS2 and IMERG6. These datasets were selected because of several reasons

179   including that they: i) have relatively high spatial resolution, ii) are gauge-adjusted products,

180   iii) are the latest products and have been found to perform well by recent studies, and iv) were

181   not compared for the basins in Ethiopia particularly IMERG6.

182   The TMPA provides rainfall products for area covering 50°N-50°S for the period of

183   1998 to present at 0.25°*0.25° and 3h spatial and temporal resolution, respectively. The 3h

184   rainfall product is aggregated to daily (3B42) and monthly (3B43) gauge-adjusted post real

185   time precipitation. The performance of the 3B42v7 is superior compared to its predecessor (i.e.,

186 3B42v6) and the real time TMPA product (3B42RT) (Yong et al., 2014). The 3B43 was used

187 in this study for the statistical evaluation while the 3B42 was used for the hydrological

188 performance evaluation. The detail description is given by Huffman et al. (2007).

189   TAMSAT3 algorithm estimates precipitation in an indirect method using cloud-index

190 method, which compares the cold cloud duration (CCD) with predetermined temperature

191 threshold. The CCD is the length of time that a satellite pixel is colder than a given temperature

192 threshold. The algorithm calibrates the CCD using parameters that vary seasonally and spatially

193 but constant from year to year. This makes interannual variations in rainfall to depend only on

194 the satellite observation. The dataset covers the whole Africa at ~4 km and 5-day (pentadal)

195 resolutions for the period of 1983 to present. The original 5-day temporal resolution is

196 disaggregated to daily time-step using daily CCD from which monthly data are derived.

197 TAMSAT3 algorithm are improved compared to its processor (i.e., TAMSAT2). The detail is

198 described in Maidment et al. (2017).

199   The Climate Hazards Group InfraRed Precipitation with Stations (CHIRPS) is a quasi-

200 global precipitation product with ~5km (0.05°) spatial resolution and is available at daily,

201 pentadal (5-day) and monthly timescales. The CHIRPS precipitation data is available from

202 1981 to present. It is gauge-adjusted dataset, which is calculated using weighted bias ratios

203 rather than using absolute station values, which minimizes the heterogeneity of the dataset

204 (Dinku et al., 2018). The latest version of CHIRPS that uses more station data (i.e., CHIRPS

205 version 2 here after CHIRPS2) was used in this study. Detail description of CHIRIPS2 is given

206 in Funk et al. (2015).

207   The Global Precipitation Measurement (GPM) is the successor of TRMM with better

208 rainfall detection capability. GPM provides precipitation measurements at $0.1°$ and half-hourly

209 spatial and temporal resolution. Integrated Multi-satellitE Retrievals for GPM (IMERG) is one

210 of the GPM precipitation product estimated from all constellation microwave sensors, IR-based

211 observations from geosynchronous satellites, and monthly gauge precipitation data. IMERG is

212 the successor algorithm of TMPA. The IMERG products includes Early Run (near real-time

213 with a latency of 6h), Late Run (reprocessed near real-time with a latency of 18 h) and Final

214 Run (gauge-adjusted with a latency of four months). The IMERG Final Run product provides

215 more accurate precipitation information compared to the near-real time products as it is gauge-

216 adjusted. The latest release of GPM IMERG Final Run version 6B (IMERG6) was used for

217 this study. The detail is given by Huffman et al. (2014).

In this study, the performances of 3B42/3, TAMSAT3, CHIRPS2 and IMERG6 rainfall products were evaluated statistically and hydrologically. All the SREs considered in this study are gauge-corrected, and thus bias correction may not be required. Thus, rain gauge stations (e.g., Jimma and Nekemte) that were used for calibrating the SREs datasets were excluded for fair comparison. The lists of rain gauge stations used for this study are shown in Figure 1 and Appendix Table 1. The detail summaries of the data types used for this study are shown in Table 1.

2.3. Methodology

Satellite rainfall estimates offer several advantages compared to the conventional methods but can also be prone to multiple errors. Rainfall detection capability of SREs can be affected by local climate and topography (Xue et al., 2013; Meng et al., 2014). Therefore, performance of SREs should be examined for a particular area before using the products for any application (Hu et al., 2014; Toté et al., 2015; Kimani et al., 2017).

The two common SREs performance evaluation methods are statistical (i.e., ground-truthing) and hydrological modelling performance (Behrangi et al., 2011; Bitew and Gebremichael, 2011; Thiemig et al., 2013, Abera et al., 2016; Jiang et al., 2017), and were used in this study. The methods complement each other and their combined application is recommended for more reliable SREs evaluation techniques. The statistical evaluation method involves pairwise comparison of SREs and the rain gauge products. The method provides insight into the intrinsic data quality whereas the modelling approach assesses the usefulness of the data for a desired application (Thiemig et al., 2013). Statistical evaluation was performed for all the SREs products considered in this study (i.e., 3B43, CHIRPS2, TAMSAT3 and IMERG6) to examine their rainfall detection skills. Continuous and categorical validation indices were used to evaluate performance of the products. In addition, the SREs product and gauge datasets were independently used as forcing to calibrate and verify SWAT model. Accordingly, streamflow prediction performance of the rainfall products was evaluated graphically and using statistical indices.

2.3.1. Statistical evaluation of satellite rainfall estimates

Statistical SREs evaluation method was conducted at monthly, seasonal and annual timescales for the overlapping period of all the rainfall data sources (i.e., 2001-2014). A daily

248 comparison was excluded from this study due to weak performance reported in previous studies

249 (Ayehu et al., 2018; Zhao et al., 2017; Li et al., 2018). This is attributed to the measurement

250 time mismatch between ground and satellite rainfall products.

251   Two approaches are commonly used for the statistical evaluation method. The first

252 approach is pixel-to-pixel pairwise comparisons of the spatially interpolated gauge-based and

253 satellite-based data. The second approach is point-to-pixel pairwise comparison where satellite

254 rainfall estimates are extracted for each gauge locations and the satellite-gauge data pairs are

255 generated and compared. The second approach was used for this study. This is because the 12

256 rainfall stations considered in this study are unevenly distributed throughout the basin to

257 accurately represent spatial variability of rainfall in the DRB as required for the first approach.

258 As a result, we chose to extract gauge-satellite rainfall pair values at each rain gauge location

259 instead of interpolating the gauge measurements into gridded products.

260   Accordingly, 168 and 2016 paired data points were extracted for annual and monthly

261 analysis, respectively, and were evaluated using continuous validation indices such as Pearson

262 correlation coefficient (r), bias ratio (*BIAS*), Nash-Sutcliffe efficiency (E) and Root Mean

263 Square Error (*RMSE*). The Pearson correlation coefficient (r) evaluates how well the estimates

264 correspond to the observed values; *BIAS* reflects how the satellite rainfall estimate over- or

265 under-estimate the rain gauge observations; E shows how well the estimate predicted the

266 observed time series. On the other hand, *RMSE* measures the average magnitude of the estimate

267 errors. The summary of performance indices are presented in Table 2.

268

269   Table 2. SREs evaluation indices, mathematical descriptions and perfect score.

Indices	Mathematical expression	Description	Perfect score
Pearson correlation	$r = \dfrac{\sum(R_g - \overline{R_g})\,(R_s - \overline{R_s})}{\sqrt{\sum(R_g - \overline{R_g})^2}\,\sqrt{\sum(R_s - \overline{R_s})^2}}$	R_g is gauge rainfall observation; R_s satellite rainfall estimates; $\overline{R_g}$ is average gauge rainfall observation; $\overline{R_s}$ is average satellite rainfall estimates. The value ranges from -1 to 1.	1
Root mean square error (mm)	$RMSE = \sqrt{\dfrac{\sum(R_g - R_s)^2}{n}}$	n is the number of data pairs; the value ranges from 0 to ∞	0
Bias ratio (BIAS)	$BIAS = \dfrac{\sum R_s}{\sum R_g}$	A value above (below) 1 indicates an aggregate satellite overestimation (underestimation) of the ground precipitation amounts.	1
Relative bias (RB)	$RB = \dfrac{\sum(R_s - R_g)}{\sum R_g} * 100$	Describes the systematic bias of the SREs; positive values indicate overestimation while negative values indicate underestimation of precipitation amounts.	0
Mean Error (ME)	$ME = \dfrac{1}{n}\sum_{i=1}^{n}(R_s - R_g)$	Describes the average errors of the SREs relative to the observed rainfall data.	0
Nash-Sutcliffe of efficiency coefficient (E)	$E = 1 - \dfrac{\sum(R_s - R_g)^2}{\sum(R_g - \overline{R_g})^2}$	The value ranges from $-\infty$ to 1; $0 < E \leq 1$ acceptable while $E \leq 0$ is unacceptable	1
Percent bias (%)	$PBIAS = \dfrac{\sum(Q_O - Q_s)}{\sum(Q_O)} * 100$	Q_O is observed discharge; Q_s is simulated discharge for the available pairs of data where $< \pm 15\%$ is very good	0
Coefficient of determination (r^2)	$r^2 = \left(\dfrac{\sum_{i=1}^{n}(O_i - \overline{O})(S_i - \overline{S})}{\sqrt{\sum_{i=1}^{n}(O_i - \overline{O})^2}\,\sqrt{\sum_{i}^{n}(S_i - \overline{S})^2}}\right)^{\wedge}2$	O_i & $\overline{O}$ is observed & average streamflow, respectively; S_i & $\overline{S}$ is simulated and average, respectively. The value ranges from 0 to 1.	1
Nash-Sutcliffe coefficient of efficiency	$NSE = \dfrac{\sum(Q_o - \overline{Q_o})^2 - \sum(Q_o - Q_s)^2}{\sum(Q_o - \overline{Q_o})^2}$	$\overline{Q_o}$ is mean value of the observed discharge for the entire time under consideration	1

270   In addition to the continuous validation indices, tercile categories (i.e., percentile-based

271   evaluation) along with probability of exceedance were performed to test the performance of

272   SREs in detecting low-and high-end values. The tercile (percentile) and probability of

273   exceedance methods better evaluates rainfall detection capabilities of SREs for monthly time

274   scale compared to the other categorical indices such as probability of detection (*POD*), false

275   alarm ratio (*FAR*) and critical success index (*CSI*). This is because the *POD*, *FAR* and *CSI* are

276   not effective for monthly-based analysis but effective for daily-based analysis.

Tercile is a set of data that are partitioned in to three equal groups each containing one-third of the total data. To calculate terciles, percentiles were used for this study. Accordingly, the low, middle and high terciles were defined using the 33th, 67th and 100th percentiles. As such, the first 33 percentile is named as lower tercile (P33), the second 33 percentile is names as medium tercile (P67) and the third 33 percentile is named as higher tercile (P100). On the other hand, probability of exceedance was calculated as a percentage of a given events to be equated or exceeded.

$$P = \frac{m}{n+1} * 100 \qquad (1)$$

where P represents the percentage probability that a given event will be equaled or exceeded

m represent ranks of the event value, with 1 being the largest possible value.

n total number of events or data points on records.

In general, SREs with r>0.7 and relative bias (RB) within 10% can be considered as reliable precipitation measurement sources (Brown, 2006; Condom et al., 2011). However, attention should be given to certain indices depending on the application of the product (Toté et al., 2015). For flood forecasting purpose, for example, underestimation of rainfall should be avoided (i.e., mean error (ME)>0 is desirable). In contrast, for drought monitoring, overestimation must be avoided (i.e., ME<0 is preferred) (Dembélé and Zwart, 2016).

2.3.2. SWAT model setup

Soil and Water Assessment Tool (SWAT) is a semi-distributed, deterministic and continuous simulation watershed model that simulates many water quality and quantity fluxes (Arnold et al., 2012). It is a physically based and computationally efficient model that has been widely used for various hydrological and/or environmental application in different regions of the world (Gassman et al., 2014). Furthermore, the capability of SWAT model to be easily linked with calibration, sensitivity analysis and uncertainty analysis tools (e.g., SWAT-CUP) made it more preferable.

SWAT model follows a two-level discretization scheme: i) sub-basin creation based on topographic data and ii) Hydrological Response Unit (HRU) creation by further discretizing the sub-basin based on land use and soil type. HRU is a basic computational unit assumed to be homogeneous in hydrologic response. Hydrological processes are first simulated at the HRU level and then routed at the sub-basin level (Neitsch et al., 2009). The SWAT model estimates

surface runoff using the modified United States Department of Agriculture (USDA) Soil Conservation Service (SCS) curve number method. In this study, a minimum threshold area of 400 km^2 were used for determining the number of sub-basins and 5% threshold for the soil, slope, and land use were used for the HRU definition. Accordingly, 13 sub basins and 350 HRUs are created for the Arjo gauging station as outlet.

2.3.3. SWAT model calibration and validation

Hydrologic modelling performance evaluation technique is commonly performed by either calibrating the hydrologic model with gauge rainfall data and then validating with SREs, (i.e., static parameters) or calibrating and validating the model independently with each rainfall products (i.e., dynamic parameters) and then compare accuracies of the streamflow predicted using the capacity of the rainfall products. The latter is preferred for watersheds such as the DRB where gauging stations are sparse and unevenly distributed. Moreover, studies have reported that independently calibrating the hydrologic model with SREs and gauge data improves performance of the hydrological model (Zeweldi et al., 2011; Vernimmen et al., 2012; Lakew et al., 2017).

Calibration, validation and sensitivity analysis of SWAT was done using the SWAT-CUP software. The Sequential uncertainty fitting (SUFI-2) implemented in SWAT-CUP was used in this study (Abbaspour et al., 2007). SUFI-2 provides more reasonable and balanced predictions than the generalized likelihood uncertainty estimation (GLUE) and the parameter solution (ParaSol) methods (Zhou et al., 2014; Wu and Chen et al., 2019) offered by the tool. It also estimates parameter uncertainty attributed to input data, and model parameter and structure as total uncertainty (Abbaspour, 2015). The total uncertainty in the model prediction is commonly measured by P-factor and *R*-factor. *P*-factor represents the percentage of observed data enveloped by the 95 percent prediction uncertainty (95PPU) simulated by the model. The *R*-factor represents the ratio of the average width of the 95PPU band to the standard deviation of observed data. For realistic model prediction, *P*-factor ≥0.7 and *R*-factor ≤1.5 is desirable (Abbaspour et al., 2007, Arnold et al., 2012).

The first steps in SWAT model calibration and validation process is determining the most sensitive parameters for a given watershed. For this study, 19 parameters were identified based on the recommendations of previous studies (Roth et al., 2018; Lemann et al., 2019). Global sensitivity analysis was performed on the 19 parameters from which 11 parameters were

338   found sensitive for the DRB, and were used for calibration, verification, and uncertainty

339   analysis. The hydrologic simulations were performed for the 2001 to 2014 period. Two years

340   of spin-up (warm-up) period (i.e., 2001 and 2002), and 6 years of calibration period (2003 to

341   2008), and 6 years of verification periods (2009 to 2014) were used. Graphical and statistical

342   measures were used to evaluate prediction capability of the rainfall datasets. Accordingly, the

343   performance of model forced by each rainfall datasets was tested using the most widely used

344   statistical indices (i.e., R^2, NSE and $PBIAS$), in addition to the P-factor and R-factor.

345   **3. Results**

346   **3.1. Statistical evaluation**

347   Figure 2 compares mean annual spatial rainfall distributions of the DRB. Average

348   annual rainfall of the study area for the 2001 to 2014 period was 1682.09 mm/year (1150 to

349   2127 mm/year), 1698.59 mm/year (1432 to 1837 mm/year), 1699.06 mm/year (1092 to 2414

350   mm/year) and 1680.28 mm/year (1342 to 1721 mm/year) according to the CHIRPS2, IMERG6,

351   TAMSAT3 and 3B43 products, respectively. For reference, mean annual rainfall for the DRB

352   is 1650 mm/year based on the rain gauge data, which is within 1.8% to 3% of the estimates

353   provided by the products. However, total annual rainfall range estimates were substantially

354   different among the products. The decreasing rainfall trend from the southern (highlands) to

355   the northern (lowlands) part of the basin were captured by all products. In particular,

356   TAMSAT3 and CHIRPS2 captured the rainfall variability in better detail, perhaps due to their

357   high spatial resolution. On the other hand, resolution of the 3B43 rainfall product seems too

358   coarse to satisfactorily represent spatial variability of rainfall in the basin.
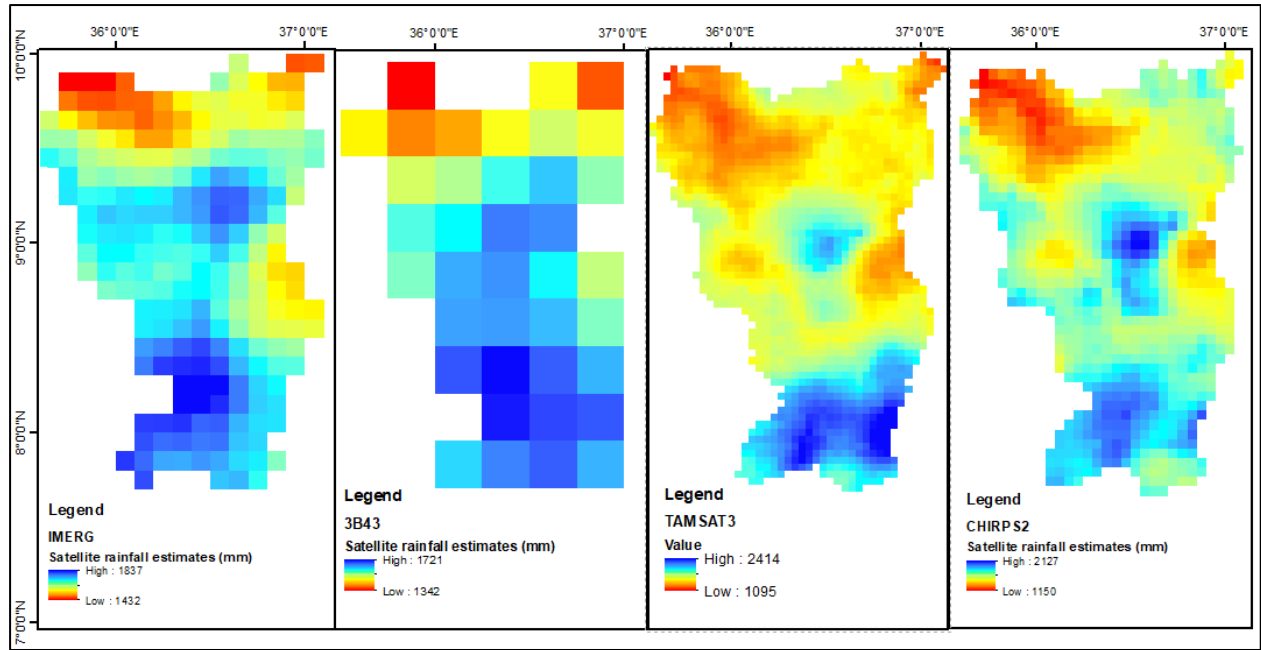
Figure 2. Spatial mean annual rainfall distribution of the four SREs for DRB (2001 to 2014)

Figures 3 to 5 show results of statistical evaluation indices calculated from rainfall from the rain gauges and from the SREs products. More specifically, Figures 3 and 4 show correlation coefficients for the annual and monthly timescales, respectively. The results show that all four SREs products produced rainfall that correlate better to the ground based rainfall observations at monthly timescale than at annual time scales. This is because performance of SREs improved with increased time aggregation and peaks at monthly timescale. More likely, the seasonal variability is much larger than the interannual variability. The seasonal variability is, apparently, captured reasonably well, causing a higher degree of correlation for monthly data. The values of statistical evaluation indices for all products are summarized in Table 3. The results show that the CHIRPS2 performed better for the DRB with relatively higher *r* and *E*, and lower *BIAS*, *ME* and *RMSE* for annual and monthly timescales, respectively.

Table 3. Statistical evaluation indices of all SREs.

SREs	*R*		*BIAS*		*ME*		*RMSE* (mm)		*E*	
	Annual	Monthly	Annual	Monthly	Annual	Monthly	Annual	Monthly	Annual	Monthly
CHIRPS2	0.78	0.92	1.01	1.01	25.94	2.70	214.36	50.48	0.51	0.84
3B43	0.48	0.87	1.02	1.02	30.58	2.55	306.34	62.05	0.76	0.76
IMERG6	0.52	0.90	1.03	1.03	48.87	4.07	299.55	56.95	0.39	0.80
TAMSAT3	0.62	0.89	1.03	1.03	51.46	2.67	274.00	61.28	0.77	0.77
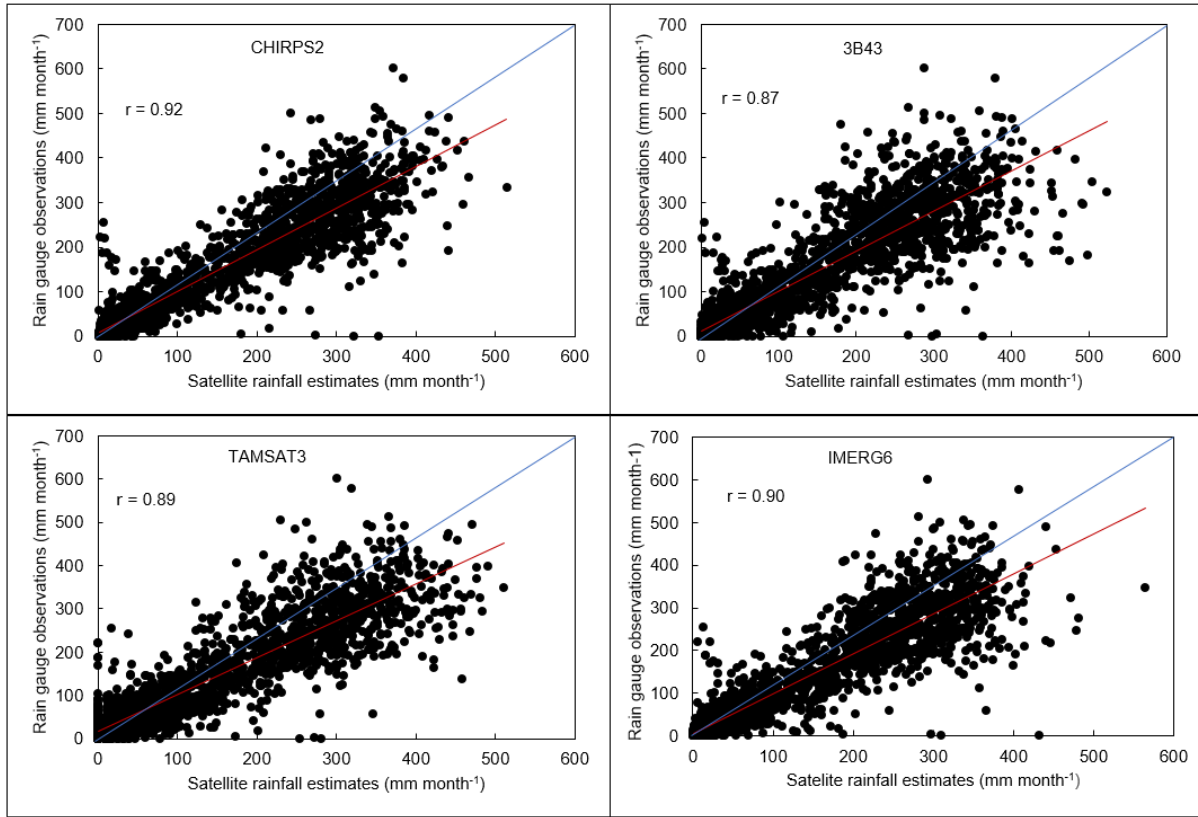
Figure 3. Correlation coefficient of the four SREs at monthly timescale over DRB.

Figures 3 to 5 and Table 3 show that generally, CHIRPS2 performed better than the other three products for the DRB. Correlation coefficients for both monthly and annual timescales as well as all the indices presented in Figure 5 favor CHIRPS2 indicating its superior performance. Relative performance of the other three SREs is inconsistent as it varies with the statistical indices used in this study. The 3B43 product, for example, performed worse based on Figure 3 and 4 (i.e., correlation coefficients for annual and monthly timescales) and *RMSE* and *E* (Figure 5), but performed better than the other two SREs based on *BIAS* and *ME*.

382
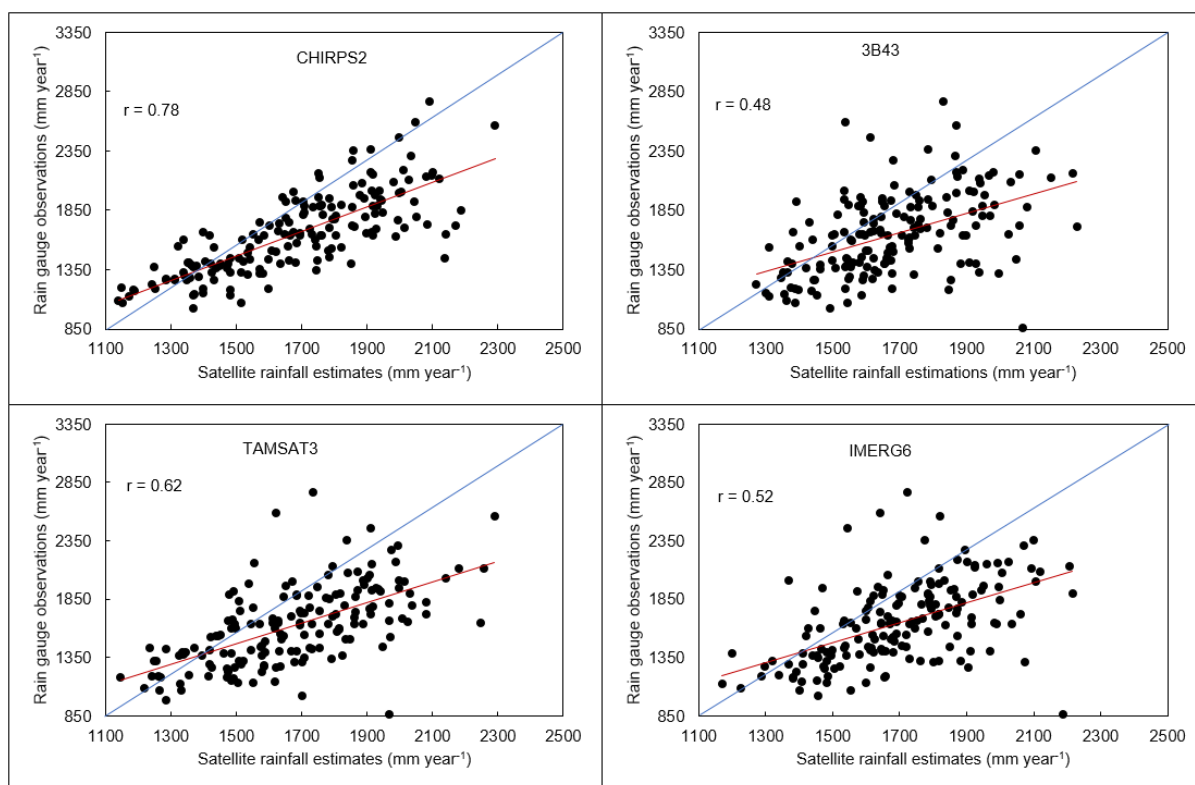
383   Figure 4. Annual correlation coefficient of the four SREs for the DRB.

384
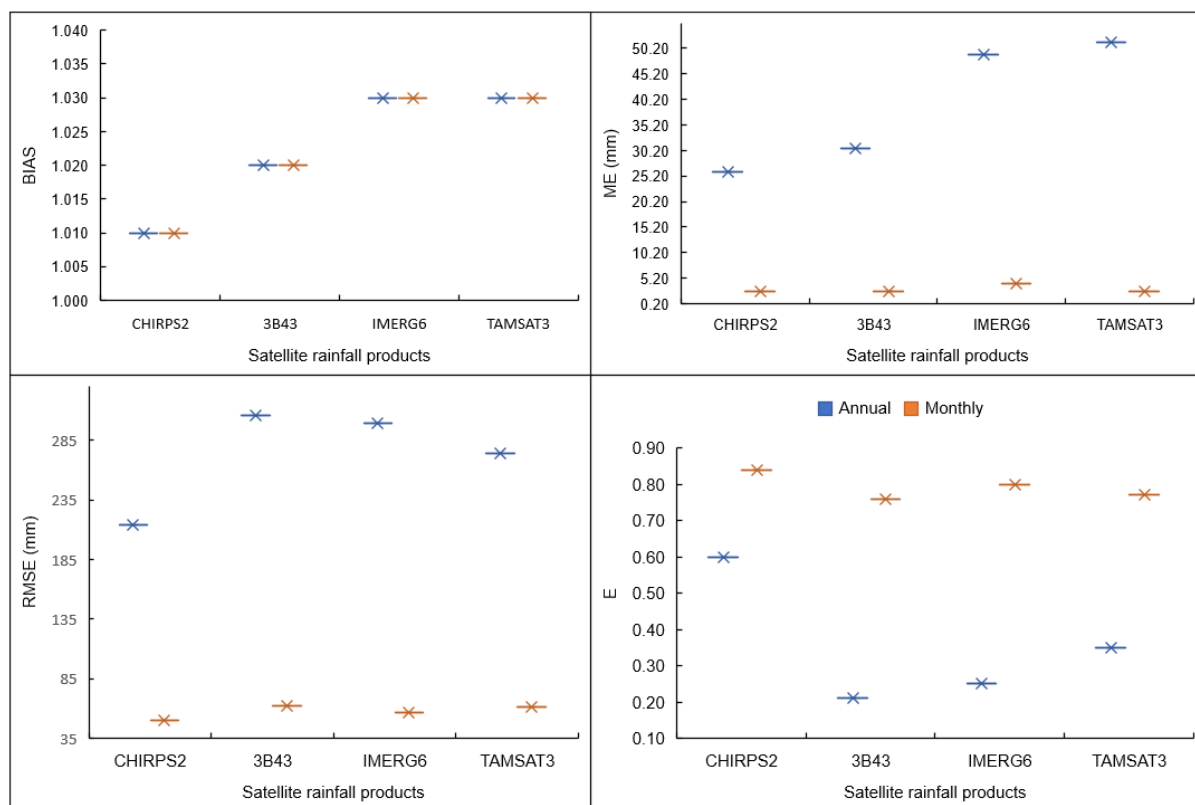
385   Figure 5. Statistical indices of the four SREs for DRB at annual and monthly time scales.

386   Tercile (percentile) categorical and probability of exceedance analysis result (Figure 6)

387 show that all the SREs considered in this study have high rainfall detection capability for the

388 DRB. Rainfall threshold used for this figure is 1mm/day. The lower tercile (33th *percentile;*

389 P33), middle tercile (67th *percentile;*P67*)* and higher tercile (100th *percentile;*P100) of all

390 SREs closer values with the corresponding gauge values indicating that the SREs detects

391 rainfall for the DRB. However, CHIRPS2, 3B43 and IMERG6 have lower tercile, medium

392 tercile and higher tercile much closer to the gauges, respectively. Moreover, the probability of

393 exceedance further confirms the rainfall detection capability of the SREs considered in this

394 study for the DRB. The probability of exceedance result indicated that TAMSAT3 has an 80%

395 probability to exceed 0 mm, whereas the other products have near 100% probability. This is

396 because TAMSAT3 has more observations with zero rainfall values compared to the other

397 products. Overall, TAMSAT3 exhibited relatively less rainfall detection skill, which could be

398 attributed to the relatively more sensitivity of TAMSAT3 to topographic effects.

399
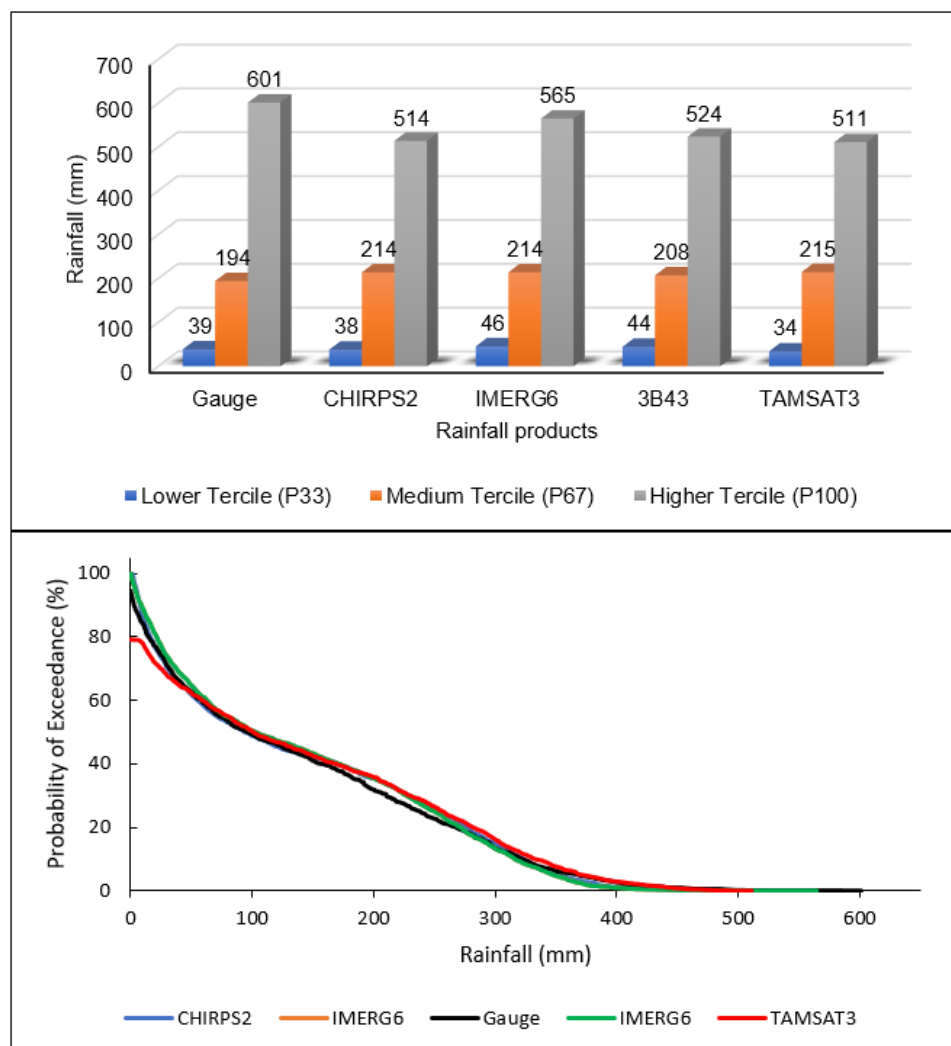
400   Figure 6. Tercile categories (top) and probability of exceedance of SREs.

Figure 7 shows seasonal SREs performance evaluation results. The figure generally shows that performance of the SREs varied from season to season and among the rainfall products. Main rainy season in the DRB is from June to September while short rainy season ranges from March to May but the rest is dry season (Figure 9). For example, CHIRPS2 is superior in detecting and estimating rainfall events for the DRB for all months (seasons). The rainfall detection and estimating capability of CHIRPS2 is better for rainy season compared to the dry season. Likewise, the rainfall detection capability of TAMSAT3 is stronger for the rainy season (May to November) but weaker for the dry season (December to April). Compared to the other SREs products, TAMSAT3 generally poorly correlated for all months (seasons), and its *BIAS* was the highest for rainy season but the lowest for the dry season.
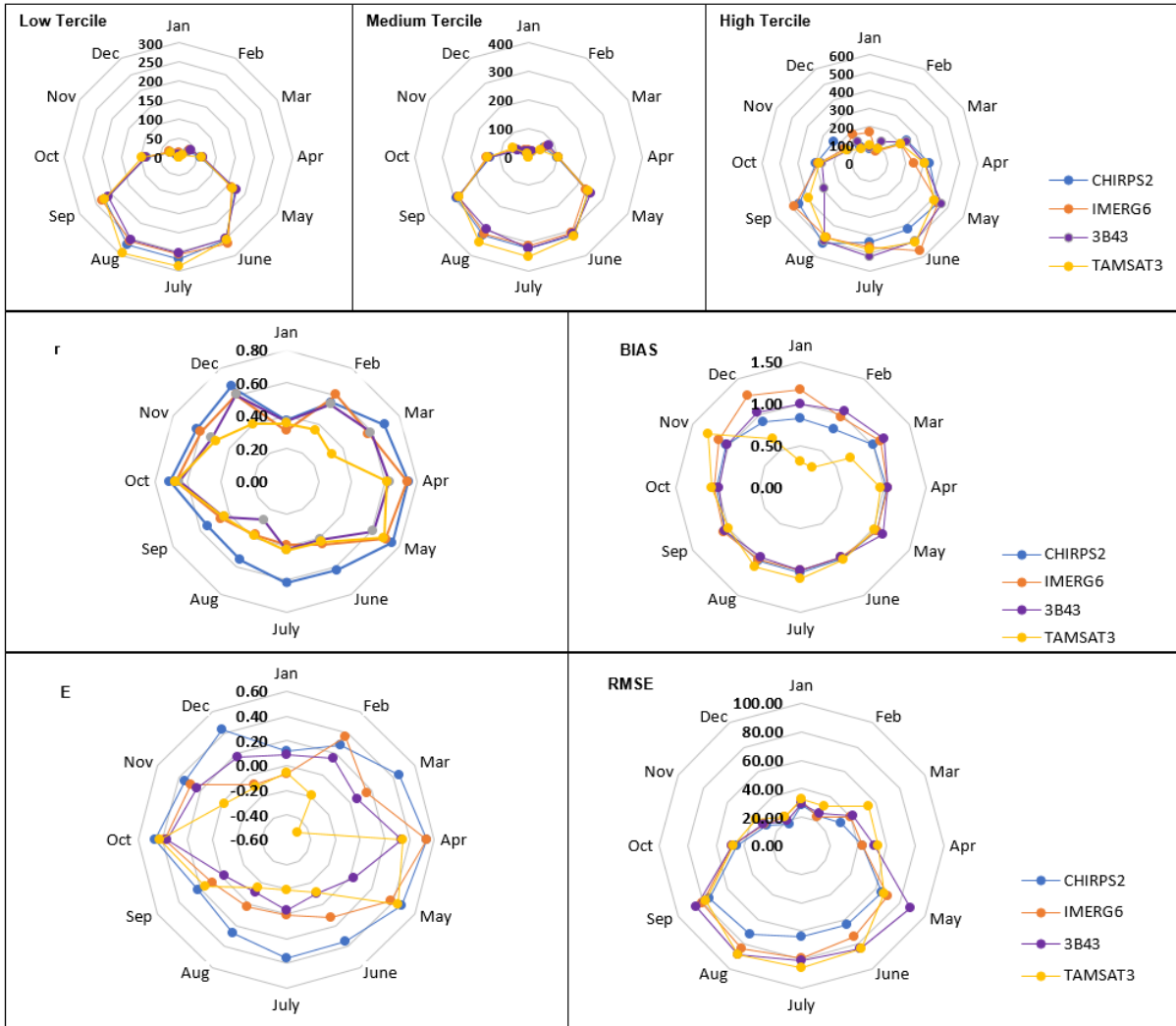
Figure 7. Seasonal statistical evaluation result comparison of each SREs for the DRB.

3.2. Hydrological modelling performance evaluation

The centroid of each sub basins were used as gauging locations, and used for extracting rainfall for all the SREs rainfall datasets. Thus, each sub basins are represented by a separate and dense gauges unlike that of the measured rainfall representation. The performance of the rainfall products were evaluated using SWAT-CUP at monthly time steps.

Table 4 shows details of the calibrated parameters including their ranges, best fit values, sensitivity ranks when different rainfall datasets are used as inputs for the DRB. The best fit values were multiplied by (1+ given value) and replaced by the given value for the parameters with *r*-prefix and *v*-prefix, respectively. The table shows that ranges and the best fit values vary from rainfall data source to another. This indicates the sensitivity of hydrological model performance to rainfall products and thus accurate characterization of rainfall variability is very critical for reliable hydrological predictions. This finding is consistent with studies that reported that different precipitation datasets influence model performance, parameter estimation and uncertainty in streamflow predictions (Sirisena et al., 2018; Goshime et al., 2019). Relative sensitivity of the parameters also varied between the rainfall datasets. In general, threshold depth of water in the shallow aquifer required for return flow to occur (mm) *(GWQMN.gw)*, base flow alpha factor *(ALPHA_BF.gw)*, Groundwater delay (day) *(GW_DELAY.gw)*, deep aquifer percolation fraction *(RCHRG_DP.gw)*, and runoff curve number for moisture condition II *(CN2.mgt)* are top five sensitive parameters. This seems indicate that groundwater processes dominate streamflow in the DRB. This could be attributed to the dominantly deep and permeable soil, vegetated land surface and dominant tertiary basaltic rocks in the DRB (Conway, 2000; Kabite and Gessesse, 2018). The groundwater parameters can have a strong effect on the amount of streamflow that can cause over or underestimation of streamflow. For this reason, the validation of streamflow was sorely dependent on the rainfall products.

Table 4. Initial parameter ranges, fit values, and sensitivity ranks for rainfall data sources.

Parameters	Initial values	Gauge		CHIRPS2		IMERG6		3B42		TAMSAT3	
		Fit value	Rank	Fit value	Rank	Fit value	Rank	Fit value	Rank	Fit value	Rank
v_GWQMN.gw	0 to 5000	4936.02	1	201.64	3	3379.76	3	4784.74	1	-0.15	1
v_ALPHA_BF.gw	0 to 1	0.00	2	0.45	4	0.04	4	0.00	2	0.00	2
v_GW_DELAY.gw	0 to 500	339.10	3	29.02	5	34.76	6	391.13	4	318.08	3
v_RCHRG_DP.gw	0 to 1	0.02	4	0.44	7	0.04	5	0.30	3	0.04	4
r_CN2.mgt	-0.25 to 0	310.12	5	-0.25	11	-0.17	10	-0.13	5	-0.15	5
r_SOL_K.sol	0 to 2000	260.96	6	1086.63	9	391.90	11	286.12	6	447.41	6
v_CH_N2.rte	-0.01 to 0.3	0.74	7	0.02	1	0.05	1	0.29	8	0.61	7
v-CH_K2.rte	-0.01 to 500	310.12	8	354.51	2	426.08	2	256.15	7	298.36	8
v_GW_REVAP.gw	0.02 to 0.2	0.40	9	0.15	8	0.20	8	0.26	9	0.33	10
r_SOL_AWC.sol	-0.5 to 0.5	-0.01	10	-0.49	6	-0.19	7	-0.85	10	-0.59	9
v_REVAPMN.gw	0 to 500	170.26	11	14.52	10	381.84	9	142.11	11	176.48	11

Figure 8 compares the observed and the predicted streamflows for the calibration (2003 to 2008) and verification (2009 to 2014) periods for all five rainfall datasets. Goodness of the streamflow predictions is also summarized in Table 5. The results show that the peak streamflow is underestimated for all rainfall products, including gauges, but the streamflow volume is generally overestimated. This could be due to the uncertainty of SREs for the extreme rainfall events at daily scale (Jiang et al., 2017) and SWAT model error. The overestimated streamflows could also be attributed to overestimation of rainfalls by the SREs as described in the previous sections. Generally, the indices provided in Table 4 indicate that the streamflow predictions are good for CHIRPS2, IMERG6, and satisfactory for the gauged rainfall but not for TAMSAT3 and 3B42 according to Moriasi et al. (2017) classification system. The performance of the SREs are consistent with the climatology of the products. Mean monthly rainfall from 2001 to 2014 showed that TAMSAT3 and 3B42 deviate more from observed rainfall while CHIRPS2 and IMERG6 are relatively closer (Figure 9).

454
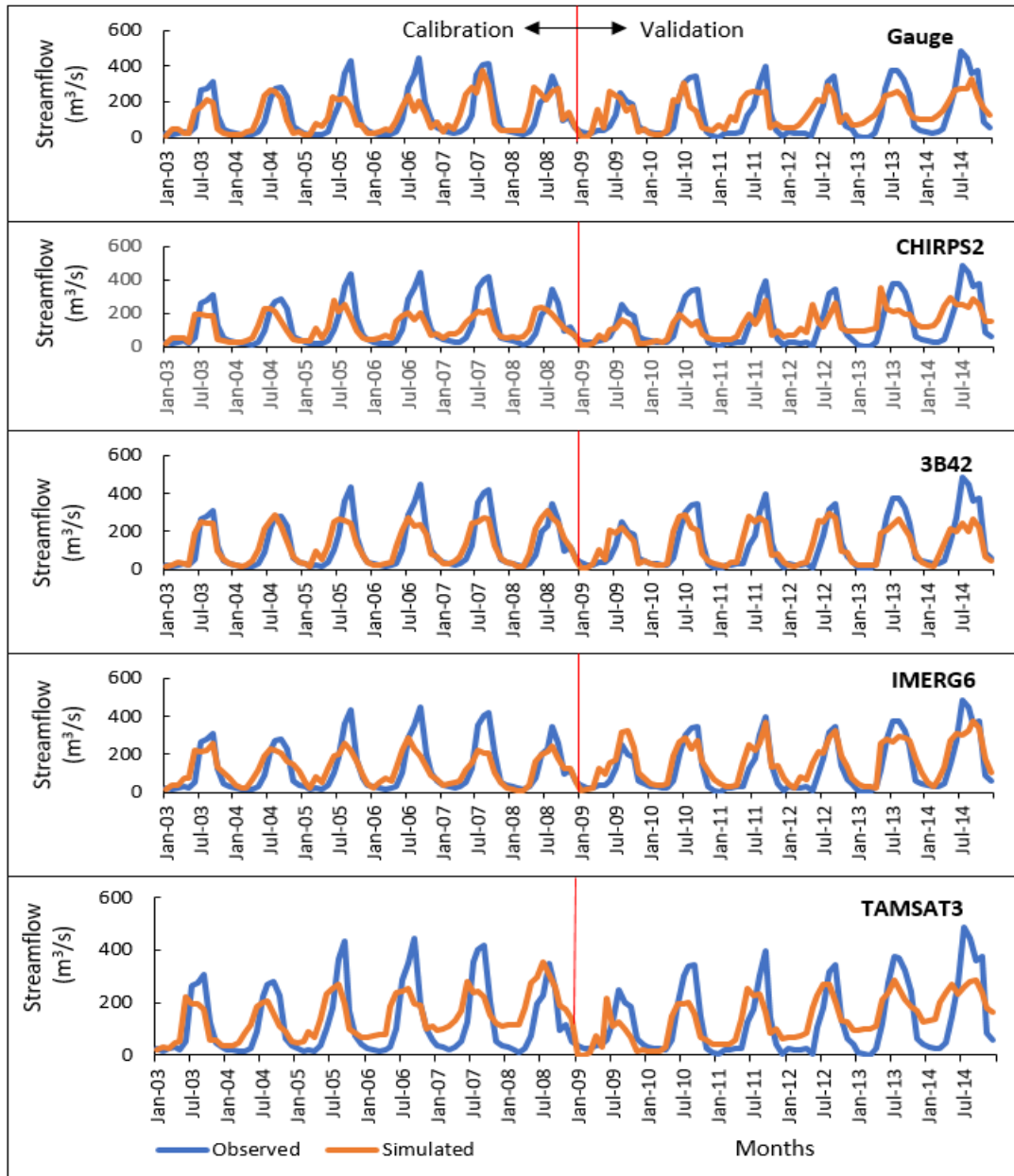
455   Figure 8. Graphical calibration and validation of streamflow at monthly scale.

456   Table 5. Calibration and validation results for the different rainfall products.

Rainfall products	Calibration					Validation				
	NSE	*R²*	*PBIAS*	*P*-factor	*R*-factor	*NSE*	*R²*	*PBIAS*	*P*-factor	*R*-factor
Gauge	0.55	0.54	2.8	0.43	0.55	0.54	0.57	-9.3	0.15	0.27
CHIRPS2	0.69	0.7	-2.5	0.72	0.64	0.65	0.66	5.3	0.46	0.58
IMERG6	0.65	0.67	2.2	0.70	0.66	0.73	0.78	-14.5	0.64	0.86
TAMSAT3	0.43	0.46	-16.7	0.31	2.94	0.48	0.48	-4.9	0.46	2.68
3B42	0.48	0.51	8.6	0.65	3.88	0.45	0.46	1.3	0.82	2.96

457
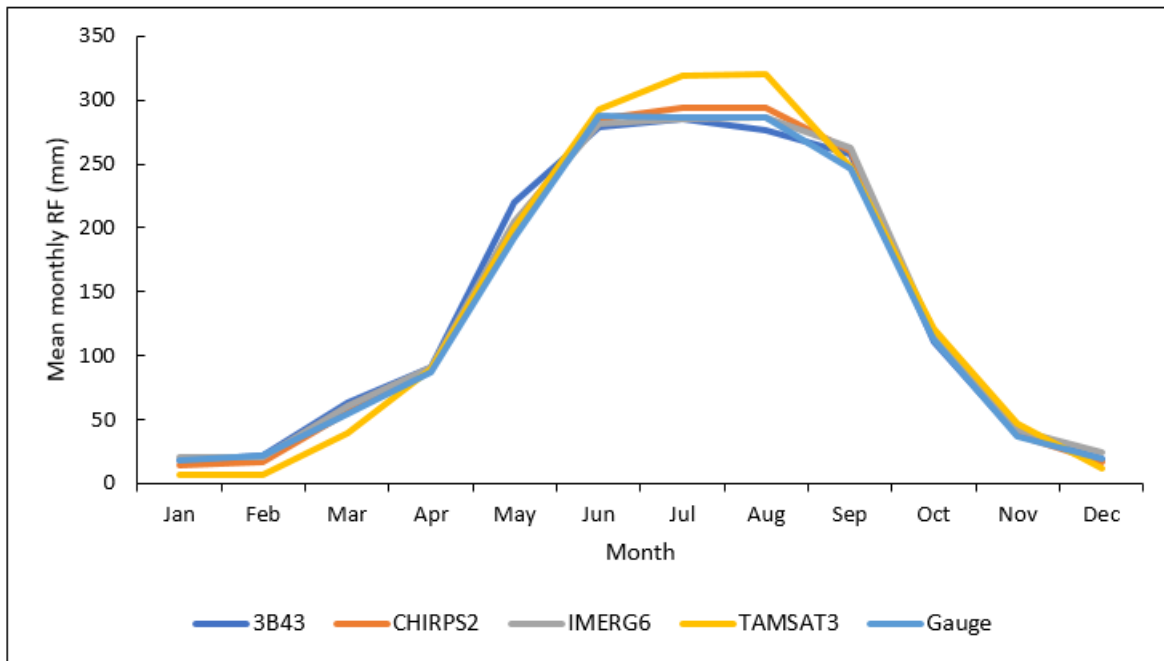
458 Figure 9. Mean monthly rainfall (2001 to 2014).

459 **4. Discussion**

460   The statistical SREs evaluation result showed that all the rainfall products captured the

461 spatiotemporal rainfall variability of the DRB except the 3B43. Poor performance of 3B43 in

462 capturing basin's rainfall variability is in agreement with findings of two previous studies done

463 for other basins in Ethiopia (Dinku et al., 2008; Worqlul et al., 2014). The reasons could be

464 attributed to the fact that gauge adjustment for 3B43 product did not use adequate gauge data

465 from Ethiopian highlands due to lack of data (Haile et al., 2013) and coarse spatial resolution

466 of the dataset (Huffman et al., 2007). However, Gebremicael et al. (2019) reported better

467 performance of 3B43 for the Tekeze-Atibara basin, which is located in the northern

468 mountainous area of Ethiopia.

469   Better correlation of SREs with observed rainfall was observed at monthly than at

470 annual timescales for all products. This is consistent with studies that reported the performance

471 of SREs improved with increased time aggregation that peaks at monthly timescale (Dembélé

472 and Zwart, 2016; Katsanos et al., 2016; Zhao et al., 2017; Ayehu et al., 2018; Li et al., 2018;

473 Guermazi et al., 2019). The weak agreement of SREs with observed data at annual timescale

474 shows that the SREs considered in this study generally did not capture the interannual rainfall

475 variability. In this regards, particularly the 3B43 product failed to capture annual rainfall

476 variability compared to the other three SREs. Overall, all four SREs products overestimated

477   rainfall for the DRB by 10% for CHIRPS2 to 30% for IMERG6 and TAMSAT3 (Figure 5).

478   This finding is consistent with studies that reported overestimation of IMERG6 and 3B43

479   products for the alpine and gorge regions of China (Chen et al., 2019). However, Gebremicael

480   et al. (2019) reported underestimation of rainfall by CHIRPS2 for the Tekeze-Atbara basin,

481   which is a mountainous and arid basin in northern Ethiopia. Ayehu et al. (2018) also reported

482   slight underestimation of rainfall by CHIRPS2 for the upper Blue Nile Basin. The discrepancy

483   between our finding and the previous studies done for the basins in Ethiopia may be due to

484   differences in watershed characteristics such as topography, vegetation cover and climatic

485   conditions.

486   Generally, this study showed that the SREs products considered in this study exhibited

487   satisfactory rainfall detection and estimation capability for the DRB. The products could be

488   applicable for flood forecasting applications for the DRB *(*Toté et al., 2015*)*. CHIRPS2

489   performed better than the other three SREs for annual, seasonal, and monthly timescales in

490   detecting and estimating rainfall for the basin. The superiority of CHIRPS2 was also reported

491   by previous studies for different parts of world (Katsanos et al., 2016; Dembélé and Zwart,

492   2016*)* including basins in Ethiopia (Bayissa et al., 2017; Ayehu et al., 2018; Dinku et al., 2018;

493   Gebremicael et al., 2019). For example, Dinku et al. (2018) reported better rainfall estimation

494   capability of CHIRPS2 for East Africa compared to African Rainfall Climatology version 2

495   (ARC2) and TAMSAT3 products. Ayehu et al. (2018) reported better performance of

496   CHIRPS2 for the Blue Nile Basin compared to ARC2 and TAMSAT3. Better performance of

497   CHIRPS2 has been attributed to the capability of the algorithm to integrate satellite, gauge and

498   reanalysis products and its high spatial and temporal resolution (Funk et al., 2015). On the

499   contrary, generally, the 3B43 rainfall product performed poorly for the DRB for all timescales.

500   This could be due to its coarse spatial resolution and lack of gauge-adjustment for highlands of

501   Ethiopia (Haile et al., 2013). The IMERG6 showed better rainfall detection and estimation

502   capability for the study area than the 3B43 product, which is consistent with findings of

503   previous studies (Huffman et al., 2015; Zhang et al., 2018; Zhang et al., 2019). Better

504   performance of IMERG6 is attributed to the inclusion of dual and high-frequency channels,

505   which improve light and solid precipitation detection capability (Huffman et al., 2015).

506   Hydrologic simulation performance evaluation result of SREs showed that accurate

507   characterization of rainfall variability is very critical for reliable hydrological predictions. This

508   finding is consistent with studies that reported that different precipitation datasets influence

509 model performance, parameter estimation and uncertainty in streamflow predictions (Sirisena

510 et al., 2018; Goshime et al., 2019). Overestimation of streamflow for all SREs products could

511 be resulted from uncertainty of SREs for extreme rainfall events at daily scale (Zhao et al.,

512 2017). The overestimated streamflow could also be attributed to overestimation of rainfalls by

513 the SREs as described in the previous sections and uncertainity of SWAT model.

514   Overall, this study showed that CHIRPS2 and IMERG6 predicted streamflow better

515 than the gauge rainfall and other two SREs products for the DRB. Superior hydrological

516 performance of SREs products compared to gauge rainfall data were also reported by many

517 other studies (Grusson et a., 2017; Bitew and Gebremichael, 2011; Goshime et al., 2019; Xian

518 et al., 2019; Li et al., 2018; Belete et al., 2020). For example, Bitew and Gebremichael (2011)

519 reported that satellite-based rainfall predicted streamflow better than gauge rainfall for complex

520 high-elevation basin in Ethiopia. Likewise, a bias-corrected CHIRP rainfall dataset resulted in

521 better streamflow prediction than a gauge rainfall dataset for Ziway watershed in Ethiopia

522 (Goshime et al., 2019).

523   The relatively poor performance of gauge rainfall compared to the CHIRPS2 and

524 IMERG6 shows that the existing rainfall gauges do not represent spatiotemporal variability of

525 rainfall in the DRB. The rain gauges are sparse, spatially uneven, and incomplete records for

526 the DRB. As previously mentioned, rain gauge density for the DRB is 0.32 per 1000 km^2,

527 which is much lower than the World Meteorological Organization (WMO) recommendation of

528 one gauge per 100-250 km^2 for mountainous areas of tropical regions such as the DRB (WMO,

529 1994).

530   In contrast to several previous studies on SREs evaluation, the present study combined

531 statistical and hydrological performance evaluation in data scarce river basin of upper Blue

532 Nile basin, the Dhidhessa River Basin. This method is important to identify SREs that better

533 detect and estimate rainfall, and select application specific rainfall products such as for

534 hydrologic and climate change studies. The results of this study also highlights seasonal

535 dependence of rainfall detection and hydrologic performance capability of SREs for DRB and

536 similar basins in Ethiopia. In addition, the performance of IMERG6, which is the latest SREs

537 product, was evaluated for Ethiopian basin for the first time. Overall, this study showed that

538 CHIRPS2 and IMERG6 rainfall products performed best in terms of detecting and estimating

539 rainfall as well as predicting streamflow for the DRB.

5. Conclusions

Satellite rainfall estimate is an alternative rainfall data source for hydrological and climate studies for data scarce regions like Ethiopia. However, SREs contain uncertainties attributed to errors in measurement, sampling, retrieval algorithm and bias correction processes. Moreover, the accuracy of rainfall estimation algorithm is influenced by topography and climatic conditions of a given area. Therefore, SREs products should be evaluated locally before they are used for any application. In this study, we examined the intrinsic data quality and hydrological simulation performance of CHIRPS2, IMERG6, 3B42/3 and TAMSAT3 rainfall datasets for the DRB. The statistical evaluation results generally revealed that all four SREs products showed promising rainfall estimation and detection capability for the DRB. Particularly, all SREs captured the south-north declining rainfall patterns of the study area. This could be due to the fact that all the SREs products were gauge adjusted and that they are the latest and improved versions. However, all the SREs datasets overestimated rainfall for DRB indicating that the rainfall products could be applicable for flood studies but not for drought studies. The result also showed strong correlation of all SREs with measured rainfall data for the monthly timescales than for the annual timescales, which shows that all the rainfall products considered in this study cannot capture interannual rainfall variability.

The quantitative statistical indices showed that CHIRPS2 performed the best in estimating and detecting rainfall events for the DRB at monthly as well as annual timescales. This is likely due to the fact that CHIRPS2 was developed by merging satellite, reanalysis and gauge datasets at high spatial resolution whereas 3B43 performed poorly for the basin.

The hydrological modelling based performance evaluation showed that ranges, best fit values, and relative sensitivities of SWAT's calibration parameters varied with the rainfall datasets. Overall, groundwater flow related parameters such as *GWQMN.gw*, *ALPHA_BF.gw*, *GW_DELAY.gw* and *RCHRG_DP.gw* were found more sensitive for all rainfall products. This showed that subsurface processes dominate hydrologic response of the DRB. The hydrological simulation performance results also showed that all the rainfall products, including the observed rainfall, overestimated streamflow especially the high flows. The peak streamflow overestimation could be attributed to the uncertainty of SREs rainfall to predict at shorter timescale (e.g., daily) and event rainfalls. The study showed CHIRPS2 and IMERG6 predicted streamflow for the basin satisfactorily, and even outperformed performance of the gauge rainfall. The relatively poor performance of the gauge rainfalls can be attributed to the fact that

572 the gauges are too sparse to accurately characterize rainfall variability in the basin. Overall,
573 CHIRPS2 and IMERG6 products seem to perform better for the DRB to detect rainfall events,
574 to estimate rainfall quantity, and to improve streamflow predictions. The new insights of this
575 study include: i) the SREs evaluation was done by combining statistical and hydrological
576 modelling methods; ii) the SREs considered in this study are the latest products reported best
577 in different studies, and IMERG6 is the most recent product evaluated in Ethiopian basin's for
578 the first time in this study and iii) the rainfall detection and estimation as well as streamflow
579 prediction capability of SREs is dependent on seasons. The results of this study are of interest
580 to both scientific communities and water resource managers, and this paper has made a good
581 contribution to improve understanding of the latest SREs for Ethiopia and the DRB. However,
582 streamflow simulation capability of the selected SREs products may be tested for other
583 hydrologic model to see if model types affect the results.

584 **Funding:** This research did not receive any specific grant from funding agencies in the public,
585 commercial, or not-for-profit sectors.

586 **Supplementary Materials:** Provided up on request.

587 **Author contributions**
588 Gizachew Kabite: Conceptualization, Data collection, analysis and interpretation, writing-
589 original draft preparation.
590 Misgana K. Muleta and Berhan Gessesse: Writing-review and editing. All authors have read
591 and agreed to the published version of the manuscript:

592 **Conflicts of Interest**

593 The authors declare no conflict of interest.

594 **Acknowledgments**

595 We are grateful to the Ethiopian Space Science and Technology Institute for providing partial
596 financial support for this research. We are also thankful to the developers of CHIRPS2,
597 IMERG6, TAMSAT3 and 3B42 datasets and for providing the data free of charge. The
598 National Meteorological Agency of Ethiopia and the Ethiopian Ministry of Water, Irrigation
599 and Energy are also acknowledged for providing climate and streamflow data, respectively.

600

References

Abbaspour, K.C.: SWAT-CUP 2012: SWAT Calibration and Uncertainty Programs-A User Manual; Swiss Federal Institute of Aquatic Science and Technology: Eawag, Switzerland. 2015.

Abbaspour, K.C., Yang, J., Maximov, I., Siber, R., Bogner, K., Mieleitner, J., Zobrist, J., and Srinivasan, R.: Modelling hydrology and water quality in the pre-alpine/alpine watershed using SWAT, J. Hydrol. 333, 413-430, 2007.

Abera, W., Brocca, L., and Rigon, R.: Comparative evaluation of different satellite rainfall estimation products and bias correction in the Upper Blue Nile (UBN) basin, Atmos. Res. 178-179,471-483, 2016.

Arnold, J.G., Moriasi,D.N., Gassman, P.W., K.C. Abbaspour, M.J. White, R. Srinivasan, C. Santhi, R.D. Harmel, A. Van Griensven, M.W., and Liew, V.: SWAT: Model use, calibration, and validation, Trans. ASABE. 55, 1491-1508, 2012.

Ayehu, G.T., Tadesse, T., Gessesse, B., and Dinku, T.: Validation of new satellite rainfall products over the Upper Blue Nile Basin, Ethiopia, Atmos. Meas. Tech. 11, 1921-1936, 2018.

Bayissa, Y., Tadesse, T., Demisse, G., and Shiferaw, A.: Evaluation of satellite-based rainfall estimates and application to monitor meteorological drought for the Upper Blue Nile Basin, Ethiopia, Remote Sens. 9,669, 2017.

Behrangi, A., Khakbaz, B., Jaw,T. Ch., Kouchak, A. A., Hsu, K. and Sorooshian, S.: Hydrologic evaluation of satellite precipitation products over a mid-size basin, J. Hydrolo. 397,225-237, 2011.

Belete, M., Deng, J., Wang, K., Zhou, M., Zhu, E., Shifaw, E., and Bayissa, Y.: Evaluation of satellite rainfall products for modeling water yield over the source region of Blue Nile Basin, Sci. Total Environ. 708,134834, 2020.

Berne, A., and Krajewski, W.F.: Radar for hydrology: Unfulfilled promise or unrecognized potential? Adv. Water Resour. 51, 357-366, 2013.

Bitew, M.M., and Gebremichael, M.: Evaluation of satellite rainfall products through hydrologic simulation in a fully distributed hydrologic model, Water Resour. Res. 47, 1-11, 2011.

631   Brown, J.E.M.: An analysis of the performance of hybrid infrared and microwave satellite

632   precipitation algorithm over India and adjacent regions. Remote Sens, Environ. 101,

633   63-81, 2006.

634   Chen, J., Wang, Z., Wu, X., Chen, X., Lai, C., and Zeng, Z., Li, J.: Accuracy evaluation of

635   GPM multi-satellite precipitation products in the hydrological application over alpine

636   and gorge regions with sparse rain gauge network. Hydrol. Res. 50, 6, 2019.

637   Condom, T., Rau, P. and Espinoza, J. C.: Correction of TRMM 3B43 monthly

638   precipitation data over the mountainous areas of Peru during the period 1998-2007,

639   Hydrol. Process. 25, 1924-1933, 2011.

640   Conway, D.: The Climate and Hydrology of the Upper Blue Nile River, The Geogr. J. 1, 49-

641   62, 2000.

642   Dembélé, M., and Zwart,S, J.: Evaluation and comparison of satellite-based rainfall

643   products in Burkina Faso, West Africa, Int. J. Remote Sens. 37(17), 3995-4014, 2016.

644   de Goncalves, L.G.G., Shuttleworth, W.J., Nijssen, B., Burke, E.J., Marengo, J.A., Chou, S.C.,

645   Houser, P., and Toll, D.L.: Evaluation of model-derived and remotely sensed

646   precipitation products for continental South America, J. Geoph. Res, 111: D16113,

647   2006.

648   Dinku, T., Chidzambwa, S., Ceccato, P., Connor, S. and Ropelewski, C.: Validation of

649   highresolution satellite rainfall products over complex terrain, Int. J. Remote Sens.,

650   29, 4097-4110, 2008.

651   Dinku, T., Funk, C., Peterson, P., Maidment, R., Tadesse, T., Gadain, H., and Ceccato., P.:

652   Validation of the CHIRPS satellite rainfall estimates over eastern Africa, Quar. J.

653   Roy. Meteo. Soci. 144, 292-312, 2018.

654   Dinku, T., Ruiz, F., Connor, S.J. and Ceccato, P.: Validation and Intercomparison of

655   Satellite Rainfall Estimates over Colombia, J. Appl. Meteorol. Climatol. 49, 1004-

656   1014, 2010.

657   Funk, C., Verdin, A., Michaelsen, J., Peterson, P., Pedreros, D. and Husak, G.: A global

658   satellite-assisted precipitation climatology, Earth Syst. Sci., Data. 7, 275-287, 2015.

659   Gassman, P.W., Sadeghi, A.M., and Srinivasan, R.: Applications of the SWAT model

660   special section: Overview and insights, J. Environ. Qual. 43, 1-8, 2014.

661   Gebremicael, T.G., Mohamed, Y.A., van der Zaag, P., Gebremedhin, M., Gebremeskel, G.,

662   Yazew, E., and Kifle, M.: Evaluation of multiple satellite rainfall products over the

663   rugged topography of the Tekeze-Atbara basin in Ethiopia, Int. J. Remote Sen.

664   40(11), 4326-4345, 2019.

665 Gebremichael, M., Bitew, M.M., Hirpa, F.A., and Tesfay, G. N.: Accuracy of satellite
666   rainfall estimates in the Blue Nile Basin: Lowland plain versus highland mountain,
667   Water Resour. Res. 50, 8775-8790, 2014.

668 Geological Survey of Ethiopia (GSE): Geology of the Nekemte and Gimbi Area. Sheet
669   Number: NC-37-9 and NC-36-12, respectively. Unpublished, 2000.

670 Goshime, D.W., Absi, R., and Ledésert, B.: Evaluation and Bias Correction of CHIRP
671   Rainfall Estimate for Rainfall-Runoff Simulation over Lake Ziway Watershed,
672   Ethiopia, Hydrology, 6:68, 2019.

673 Grusson, Y., Antil, F., Sauvage, S., and Perz, S.: Testing the SWAT Model with Gridded
674   Weather Data of Different Spatial Resolution. Water, 9:54, 2017.

675 Guermazi, E., Milano, M., and Reynard, E.: Performance evaluation of satellite-based
676   rainfall products on hydrological modelling for a transboundary catchment in northwest
677   Africa, Theo. App. Clim. 138, 1695-1713, 2019.

678 Habib, E., Haile, A. T., Tian, T., and Joyce, R. J.: Evaluation of the High-Resolution
679   CMORPH Satellite Rainfall Product Using Dense Rain Gauge Observations and Radar-
680   Based Estimates, J. Hydrmeteo., 13 (6), 1784-1798, 2012.

681 Haile, A. T., Habib, E., Elsaadani, M., and Rientjes, T.: Intercomparison of satellite
682   rainfall products for representing rainfall diurnal cycle over the Nile basin, Int. J. Appl.
683   Earth Obs. 21, 230-240, 2013.

684 Hu, Q., Yang, D., Li, Z., Mishra, A.K., Wang, Y., and Yang, H.: Multi-scale evaluation   of
685   six high-resolution satellite monthly rainfall estimates over a humid region in China
686   with dense rain gauges, Int. J. Remote Sens. 35, 1272-1294, 2014.

687 Huffman, G. J., Bolvin, D. T., Nelkin, E. J., Wolff, D. B., Adler, R. F., Gu, G., Hong, Y.,
688   Bowman, K. P., and Stocker, E. F.: The TRMM Multisatellite Precipitation
689   Analysis (TMPA): quasiglobal, multiyear, combined-sensor precipitation estimates at
690   fine scales, J. Hydrometeorol. 8, 38-55, 2007.

691 Huffman, G.J., Bolvin, D.T., Braithwaite, D., Hsu, K., Joyce, R.J., Kidd, C., Nelkin, E.J., and
692   Xie, P.: Algorithm Theoretical Basis Document (ATBD), 2015.

693 Huffman, G.J., Bolvin, D.T., Braithwaite, D., Hsu, K., Joyce, R., Xie, P., and Yoo, S.H.:
694   NASA global precipitation measurement (GPM) integrated multi-satellite retrievals
695   for GPM (IMERG). In Algorithm Theoretical Basis Document (ATBD); NASA/GSFC:
696   Greenbelt, MD, USA, 2014.

697 Jiang, S., Liu, S., Ren, L., Yong, B., Zhang, L., Wang, M., Lu, Y., and He, Y.: Hydrologic
698   Evaluation of Six High Resolution Satellite Precipitation Products in Capturing
699   Extreme Precipitation and Streamflow over a Medium-Sized Basin in China, Water,
700   10, 25, 2017.

701 Joyce, R. J., Janowiak, J. E., Arkin, P. A., and Xie, P.: CMORPH: a method that produces
702   global precipitation estimates from passive microwave and infrared data at high spatial
703   and temporal resolution, J. Hydrometeo. 5, 487-503, 2004.

704 Kabite, G., and Gessesse, G.: Hydro-geomorphological characterization of Dhidhessa
705   River Basin, Ethiopia, Int. Soil and Water Cons. Res. 6, 175-183, 2018.

706 Kabite, G., Muleta, M.K., and Gessesse, B.: Spatiotemporal land cover dynamics and
707   drivers for Dhidhessa River Basin (DRB), Ethiopia, Mod. Earth Sys. Environ. 6,
708   1089-1103, 2020.

709 Katsanos, D., Retalis, A., and Michaelides. S.: Validation of a high-resolution
710   precipitation database (CHIRPS) over Cyprus for a 30-year period, Atmos.
711   Res. 169, 459-464, 2016.

712 Kidd, C., and Huffman, G.: Global precipitation measurement. Meteorol. Appl. 18,334-
713   353, 2011.

714 Kidd, C., Bauer, P., Turk, J., Huffman, G.J., Joyce, R., Hsu, K.L., and Braithwaite, D.:
715   Intercomparison of high-resolution precipitation products over northwest Europe. J.
716   Hydrometeorol. 13, 67-83, 2012.

717 Kimani, M.W., Hoedjes, J.C.B., and Su, Z.: An assessment of satellite-derived rainfall
718   products relative to ground observations over East Africa, Remote Sens. 9(5), 430,
719   2017.

720 Lakew, H.B., Moges, S.A., and Asfaw, D.H.: Hydrological Evaluation of Satellite and
721   Reanalysis precipitation products in the Upper Blue Nile Basin: A case study of Gilgal
722   Abbay, Hydrology, 4, 39, 2017.

723 Lemann, T., Roth, V., Zeleke, G., Subhatu, A., Kassawmar, T., and Hurni, H.: Spatial and
724   Temporal Variability in Hydrological Responses of the Upper Blue Nile basin,
725   Ethiopia, Water, 11, 21, 2019.

726 Li, D., Christakos, G., Ding, X., and Wu, J.: Adequacy of TRMM satellite rainfall data in
727   driving the SWAT modeling of Tiaoxi catchment (Taihu lake basin, China), J. Hydr.
728   556, 1139-1152, 2018.

729 Maggioni, V., Meyers, P.C., and Robinson, M.D.: A Review of Merged High-Resolution
730   Satellite Precipitation Product Accuracy during the Tropical Rainfall Measuring
731   Mission (TRMM) Era, J. Hydrometeor. 17, 1101-1117, 2016.

732 Maidment, R., Emily, B., and Matt, Y.: TAMSAT Daily Rainfall Estimates (Version 3.0).
733   University of Reading. Dataset. doi.org/10.17864/1947.112, 2017.

734 Meng, J., Li, Z., Hao, J., Wang, S. Q.: Suitability of TRMM Satellite Rainfall in Driving
735   Distributed Hydrological Model in the Source Region of Yellow River. J. Hydrol.
736   509, 320-332, 2014.

737 Moriasi, D. N., Arnold, J. G., Van Liew, M. W., Bingner, R.L., Harmel, R.D., and Veith, T.L.:
738   Model evaluation guidelines for systematic quantification of accuracy in   watershed
739   simulations. Trans. American Socie. Agr. Bio. Eng. 50(3), 885-900, 2007.

740 Nebuloni, R., D'Amico, M., Cazzaniga, G., De Michele, C., and Deidda, C.: Rainfall
741   estimate using Commercial Microwave Links (CML): first outcomes of the
742   MOPRAM project. EGU2020-1040, 19th EGU General Assembly, EGU2017,
743   proceedings from the conference held 23-28 April, 2017 in Vienna, Austria., p.18576.
744   https://doi.org/10.5194/egusphere-egu2020-1040, 2020.

745   Neitsch, S.L., Arnold, J.G., Kiniry, J.R., and Williams, J.R.: Soil & Water Assessment
746   Tool-Theoretical Documentation Version 2009. Texas Water Resour. Inst, 2009.

747 Nesbitt, S.W., Gochis, D.J., and Lang, T.J.: The diurnal cycle of clouds and precipitation
748   along the Sierra Madre Occidental observed during NAME-2004: Implications for
749   warm season precipitation estimation in complex terrain, J. Hydrometeoro. 9, 728-
750   743, 2008.

751 Nguyen, T.H., Masih, I., Mohamed, Y.A., and Van Der Zaag, P.: Validating rainfall-
752   runoff modelling using satellite-based and reanalysis precipitation products in the Sre
753   Pok catchment, the Mekong River basin, Geosciences, 8(5), 164-184, 2018.

754 Oromia Water Works Design and Supervision Enterprise (OWWDSE).: Dhidhessa Sub-
755   Basin Soil Survey Report. Dhidhessa-Dabus Integrated Land Use Planning Study
756   Project. Unpublished, 2014.

757 Roth, V., Lemann, T., Zeleke, G., Subhatu, A.T., Nigussie, T.K., and Hurni, H.: Effects   of
758   climate change on water resources in the upper Blue Nile Basin of Ethiopia, Heliyon,
759   4(2018) e00771, 2018.

760 Sahlaoui, Z., and Mordane, S.: Radar Rainfall Estimation in Morocco: Quality
761 Control and Gauge Adjustment. Hydrology, 6 (2):41, 2019.

762 Smiatek, G., Keis, F., Chwala, C., Fersch, B., and Kunstmann, H.: Potential of
763   commercial microwave link network derived rainfallfor river runoff simulations.
764   Environmental Research Letter, 12, 034026, 2017.

765 Seyyedi, H., Angagnostou, E.N., Beinghley, E., and McCollum, J.: Hydrologic evaluation
766   of satellite and reanalysis precipitation datasets over a mid-latitude basin, Atm.
767   Res. 164-165, 37-48, 2015.

768 Sirisena, T.A.J.G., Maskey, S., Ranasinghe, R., and Babel, M.S.: Effects of different
769   precipitation inputs on streamflow simulation in the Irrawaddy River Basin, Myanmar.
770   J. Hyd.: Reg. Studies. 19,265-278, 2018.

771 Sorooshian, S., Hsu, K.-L., Gao, X., Gupta, H. V., Imam, B., and Braithwaite, D.: Evaluation
772   of PERSIANN system satellite-based estimates of tropical rainfall, B. Am. Meteorol.
773   Soc. 81, 2035-2046, 2000.

774 Stisen, S., and Sandholt, I.: Evaluation of remote-sensing-based rainfall products through
775   predictive capability in hydrological runoff modeling, Hydrol. Proce. 24, 879-
776   891, 2010.

777 Su, J., Lü, H., Wang, J., Sadeghi, A., and Zhu, Y.: Evaluating the Applicability of Four
778   Latest Satellite-Gauge Combined Precipitation Estimates for Extreme Precipitation
779   and Streamflow Predictions over the Upper Yellow River Basins in China. Remote
780   Sens. 9, 1176, 2017.

781 Tapiador, F.J., Turk, F.J., Petersen, W., Hou, A.Y., García-Ortega, E., Machado, L.A.T.,
782   Angelis, C.F., Salio, P., Kidd, C., Huffman, G.J., et al., Global precipitation
783   measurement: Methods, datasets and applications. Atmos. Res. 104-105, 70-97, 2012.

784 Thiemig, V., Rojas, R., Zambrano-Bigiarini, M., and Roo, A. D.: Hydrological evaluation
785   of satellite-based rainfall estimates over the Vota and Baro-Akobo Basin, J.
786   Hydrology. 499, 324-333, 2013.

787 Tong, K., Su, F., Yang, D., and Hao, Z.: Evaluation of satellite precipitation retrievals and
788   their potential utilities in hydrologic modeling over the Tibetan Plateau, J. Hydrol.
789   519, 423-437, 2014.

790 Toté, C., D. Patricio, H. Boogaard, R. Van der Wijngaart, E. Tarnavsky, and Funk, C.:
791   Evaluation of Satellite Rainfall Estimates for Drought and Flood Monitoring in
792   Mozambique, Remote Sens. 7 (2), 1758-1776, 2015.

793 Vernimmen, R.R., Hooijer, A., Aldrian, E., and Van Dijk, A.I.: Evaluation and bias
794   correction of satellite rainfall data for drought monitoring in Indonesia, Hydrol.
795   Earth Syst. Sci., 16, 133-146, 2012.

796   Villarini, G., Krajewski, W.F.: Review of the different sources of uncertainty in single
797   polarization radar-based estimates of rainfall. Surv. Geophys., 31, 107-129, 2010.

798   WMO: World Meteorological Organization Guide to Hydrological Practices: Data
799   Acquisition and Processing, Analysis, Forecasting and Other Applications. Geneva:
800   Switzerland, 1994.

801   Worqlul, A.W., Maathuis, B., Adem, A.A., Demissie, S.S., Langan, S., and Steenhuis, T.S.:
802   Comparison of rainfall estimations by TRMM3B42, MPEG and CFSR with
803   ground-observed data for the Lake Tana basin in Ethiopia, Hydrol. Earth Syst. Sci.
804   18, 4871-4881, 2014.

805   Wu, H., and Chen, B.: Evaluating uncertainty estimates in distributed hydrological
806   modeling for the Wenjing River watershed in China by GLUE, SUFI-2, and ParaSol
807   methods, Ecol. Eng. 76,110-121, 2015.

808   Xian, L., Wenqi, W., Daming, H., Yungang, L., and Xuan., J.: Hydrological Simulation
809   Using TRMM and CHIRPS Precipitation Estimates in the Lower Lancang-Mekong
810   River Basin. China Geog. Sci. 29(1), 13-25, 2019.

811   Xie, P., and Arkin, A.: An Inter-comparison of Gauge Observations and Satellite Estimates
812   of Monthly Precipitation, J. Appl. Meteoro. 34, 1143-1160, 1995.

813   Xue, X., Hong, Y., Limaye, A.S., Gourley, J.J., Huffman, G.J., Khan, S.I., and Chen, S.:
814   Statistical and Hydrological Evaluation of TRMM-Based Multi-Satellite Precipitation
815   Analysis over the Wangchu Basin of Bhutan: Are the Latest Satellite Precipitation
816   Products 3B42V7 Ready for Use in Ungauged Basins? J. Hydrol. 499, 91-99, 2013.

817   Yohannes, O.: Water Resources and Inter-Riparian Relations in the Nile Basin: The
818   Search for an integrative Discourse. 270, 2008.

819   Yong, B., Chen, B., Gourley, J.J., Ren, L., Hong, Y., Chen, X., Wang, W., Chen, S., and Gong,
820   L.: Inter-comparison of the Version-6 and Version-7 TMPA precipitation products
821   over high and low latitudes basins with independent gauge networks: is the
822   newer version better in both real-time and post-real-time analysis for water resources
823   and hydrologic ext, J. Hydrol. 508, 77-87, 2014.

824   Zeweldi, D.A., Gebremichael, M., and Downer, C.W.: On CMORPH rainfall for streamflow
825   simulation in a small, Hortonian watershed. J. Hydrometeorol. 12, 456-466, 2011.

826   Zhang, C., Chen, X., Shao, H., Chen, S., Liu, T., Chen, C., Ding, Q., and Du, H.: Evaluation
827   and Inter-comparison of High-Resolution Satellite Precipitation Eastimates-GPM,
828   TRMM, and CMORPH in the Tianshan Mountain Area. Remote sens. 10, 1543, 2018.

829 Zhang, Z., Tian, J., Huang, Y., Chen, X., Chen, S., and Duan, Z.: Hydrologic Evaluation of
830   TRMM and GPM IMERG Satellite-Based Precipitation in a Humid Basin of China.
831   Remote Sens. 11, 431, 2019.

832 Zhao, Y., Xie, Q., Lu, Y., and Hu, B.: Hydrologic Evaluation of TRMM Multisatellite
833   Precipitation Analysis for Nanliu River Basin in Humid Southwestern China. Scie.
834   Reports, 7, 2470, 2017.

835 Zhou, J., Liu, Y., Guo, H., and He, D.: Combining the SWAT model with sequential
836   uncertainty fitting algorithm for streamflow prediction and uncertainty analysis for the
837   Lake Dianchi Basin, China. Hydrol. Process. 28, 521-533, 2014.

838

839 **Appendix**

840 Appendix Table 1. List of rain gauge stations used for SREs evaluation.

S. No	Stations	Latitude	Longitude	Elevation	Remark
1	Bedele	8.3	36.2	2011	Within the basin
2	Gatira	8.0	36.2	2358	Within the basin
3	Gimbi	9.2	35.8	1970	Within the basin
4	Nedjo	9.5	35.5	1800	Within the basin
5	Anger	9.3	36.3	1350	Within the basin
6	Gida Ayana	9.9	36.9	1850	Within the basin
7	Arjo	8.5	36.3	2565	Within the basin
8	Jimma*	7.8	36.4	1718	Within the basin
9	Nekemte*	9.1	36.5	2080	Within the basin
10	Shambu	9.6	37.1	2460	Near the basin
11	SibuSire	9.0	35.9	1826	Within the basin
12	Bure	8.2	35.1	1750	Near the basin
13	Sokoru	7.9	37.4	1928	Near the basin
14	Gore	8.1	35.5	2033	Near the basin

841 *systematically removed from using for calibration as they are already used for SREs calibration.

Editors' Response

Dear editor,

Thank you very much for your very constructive comments. Your comments improved the quality of our manuscript. In response to your comments I have modified the manuscript.

Please include a few statements describing the figure to the results and discussion sections (whichever is most applicable).

Response: I have described Figure 6 to the result part (line 391-397).

Add an explanation how you calculated the terciles and the probability of exceedance.

Responses: We have included how the terciles and probability of exceedance were calculated in the methodology part (line 277-287).

Remove the statistical variables you don't use (e.g., POD and FAR) from table 2.

Response: Done